Journal of Organometallic Chemistry 694 (2009) 771–779

Contents lists available at ScienceDirect

Journal of Organometallic Chemistry

journal homepage: www.elsevier.com/locate/jorganchem

Theoretical study on the substitution and insertion reactions of silylenoid H_2SiLiF with CH_3XH_{n-1} (X = F, Cl, Br, O, N; n = 1, 1, 1, 2, 3)

Yuhua Qi [a,b], Dacheng Feng [a,*], Rui Li [a], Shengyu Feng [a]

[a] Institute of Theoretical Chemistry, School of Chemistry and Chemical Engineering, Shandong University, Jinan 250100, People's Republic of China
[b] School of Chemistry and Chemical Engineering, University of Jinan, Jinan 250022, People's Republic of China

ARTICLE INFO

Article history:
Received 17 September 2008
Received in revised form 3 December 2008
Accepted 4 December 2008
Available online 16 December 2008

Keywords:
Substitution reactions
Insertion reactions
DFT
Silylenoids
Solvent effects

ABSTRACT

The substitution and insertion reactions of H_2SiLiF (**A**) with CH_3XH_{n-1} (*X = F*, Cl, Br, O, N; n = 1, 1, 1, 2, 3) have been studied using density functional theory. The results indicate that the substitution reactions of **A** with CH_3XH_{n-1} proceed via two reaction paths, I and II, forming the same product H_2SiFCH_3. The insertion reactions of **A** with CH_3XH_{n-1} form $H_2SiXH_{n-1}CH_3$. The following conclusions emerge from this work. (i) The substitution reactions of **A** with CH_3XH_{n-1} occur in a concerted manner. The substitution barriers of **A** with CH_3XH_{n-1} for both pathways decrease with the increase of the atomic number of the element X for the same family systems or for the same row systems. Path I is more favorable than path II. (ii) **A** inserts into a C–X bond via a concerted manner, and the reaction barriers increase for the same-row element X from right to left in the periodic table, whereas change very little for the systems of the same-family element X. (iii) The substitution reactions occur more readily than the insertion reactions for **A** with CH_3XH_{n-1} systems. (iv) All substitution and insertion reactions of **A** with CH_3XH_{n-1} are exothermic. (v) In solvents, the substitution reaction process of **A** with CH_3XH_{n-1} is similar to that in vacuum. The barrier heights in solvents increase in the order $CH_3F < CH_3Cl < CH_3Br < CH_3OH < CH_3NH_2$. The solvent polarity has little effects on the substitution barriers. The calculations are in agreement with experiments.

1. Introduction

Silylenoids, R_2SiMX (X = halogen, M = alkali metal), are important intermediates in silicon hybrid and organosilicon chemistry [1,2]. Previous researches have shown that silylenoid can be regarded as a silylene complex, in which a leaving group X and a metal atom M are bound to the same silicon atom. In principle, silylenoids undergo the same type of reactions as silylenes. Recent theoretical calculations and experiments indicate the addition reactions of silylenoid [3–5] H_2SiLiX (X = F, Cl) to unsatured bonds, such as C=C, C≡C and C=O, are similar to the additions of SiH_2 [6–13] into these bonds in the reaction process, mechanisms, and final products. The insertions of silylenoid H_2SiLiX (X = F, Cl) into H_2 and Y–H (Y = C, Si, N, P, O, S, and F) [14–17] also resemble the insertions of SiH_2 into H_2 and Y–H bonds [18–21] except their different barriers.

Recently, West and coworkers reported the experimental results of the reactions of the stable silylene, *N,N′*-di-*tert*-butyl-1,3-diaza-2-silacyclopent-4-en-2-yildene, with chloro and bromocarbons in hexane [22]. In these reactions, the stable silylene has been found to insert into a C–X (X = halogen) bond of a halocarbon. Ming-Der Su studied the insertion mechanism of silylene into C–X (X = Cl, Br) bonds and found that the preference insertion of C–X over C–H as a result of the thermodynamic factor and silylenes prefer to insert into C–Br rather than C–Cl, providing the reaction conditions remain the same [23].

Gregory Molev et al. recently prepared the first fluorosilylenoid **1** by reaction of fluorobromosilane with silyllithium in THF, determined its molecular structure by X-ray crystallography, and demonstrated its versatile reactivity [24]. When **1** reacts as a nucleophile with CH_3Cl, **2**, not the insertion product **3**, forms. **2** can be regarded as the product of the Li atom in silylenoid **1** substituted by the moiety CH_3 of CH_3Cl. That is to say, **2** is the product of the substitution reaction of **1** with CH_3Cl.

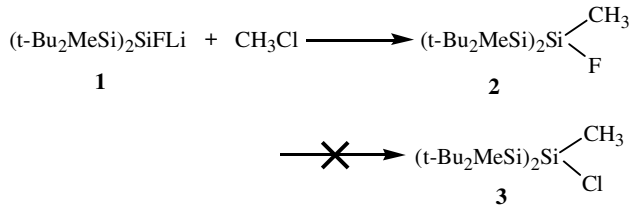

1 **2** **3**

Obvious questions are obtained from these novel experiments. Why does the reaction of **1** and CH_3Cl undergo the substitution path not an insertion path? What is the substitution mechanism of **1** with

* Corresponding author. Fax: +86 0531 88564464.
E-mail address: fdc@sdu.edu.cn (D. Feng).

0022-328X/$ - see front matter © 2008 Elsevier B.V. All rights reserved.
doi:10.1016/j.jorganchem.2008.12.017

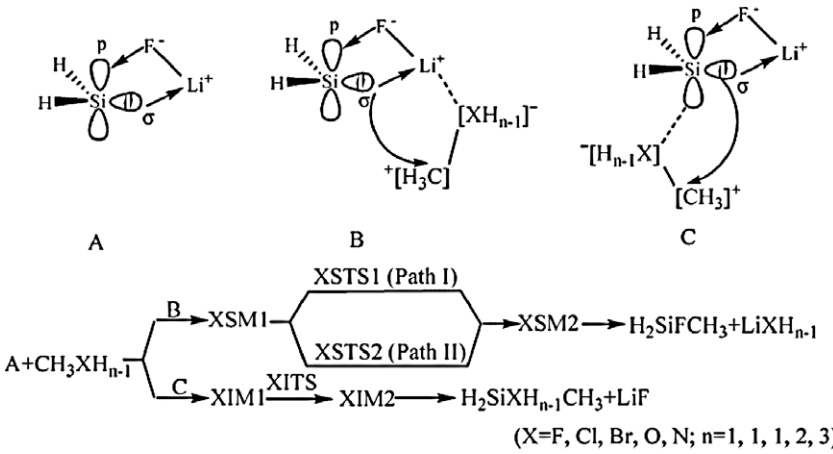

Fig. 1. The three-membered ring H_2SiLiF (A) and its substitution (B) and insertion (C) reaction paths with CH_3XH_{n-1} (X = F, Cl, Br, O, N; n = 1, 1, 1, 2, 3).

CH_3Cl? To get insight on these questions and examine the generality of the silylenoid insertion and substitution reactions, we have investigated the reactions of silylenoids with CH_3XH_{n-1} (X = F, Cl, Br, O, N; n = 1, 1, 1, 2, 3) using density functional theory. The simple model H_2SiLiF, which has the similar structure and same reaction center with $(t\text{-}Bu_2MeSi)_2SiFLi$, is adopted in this study. Through this theoretical work, we hope (i) to clarify the reaction mechanisms and to determine the structures and energies of all stationary points, (ii) to investigate the thermodynamics of these insertion and substitution reactions, (iii) to estimate their activation barriers and to understand the origin of the barriers heights, (iv) to establish general trends and predictions for the insertion and substitution reactions of silylenoids with C–X bonds, (v) to compare the insertion with the substitution and build an order of priority of silylenoid insertion and substitution reactions with CH_3F, CH_3Cl, CH_3Br, CH_3OH, and CH_3NH_2 molecules, and (vi) to reveal the solvent effects on the reactions of silylenoids with CH_3XH_{n-1} (*X = F,* Cl, Br, O, N; n = 1, 1, 1, 2, 3).

2. Theoretical methods

Optimized geometries for the stationary points were obtained at the B3LYP/6-311+G (d, p) [25–28] level. The corresponding harmonic vibrational frequency calculations were carried out in order to characterize all stationary points as either local minima (no imaginary frequencies) or transition states (one imaginary frequency). Based on the optimized geometries, energies were obtained and natural bond orbital (NBO) [29–31] analyses were then used to study the nature of different interactions between atoms and groups. The reaction paths were examined by intrinsic reaction coordinate (IRC) [32] calculations. The solvent effects, which were simulated using the self-consistent reaction field (SCRF) method with Tomasi's polarized continuum model (PCM) [33–42], were investigated at the same level. GAUSSIAN 03 [43] series of programs were employed in all calculations.

3. Results and discussion

Previous calculations have shown that each silylenoid R_2SiMX has four equilibrium isomers, the three-membered-ring, the p-complex, the σ-complex, and the 'classical' tetrahedral structures [44–47]. The three-membered ring structure is the most stable and possibly detectable one in chemical reactions [48,49]. Additionally, the structure of fluorosilylenoid **1** determined by X-ray crystallography is also analogue to the three-membered ring structure silylenoid [24]. So the three-membered-ring structure of H_2Si-LiF (marked as **A**, see Fig. 1) is adopted for this study. NBO analysis indicates that the main part of HOMO in **A** is the Si atom, and a part of LUMO is the p-orbital on the Si atom though the main part of LUMO is localized on the Li atom.

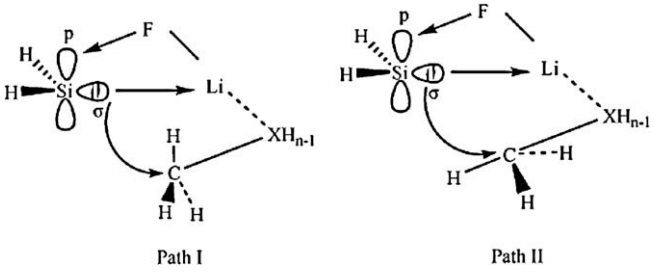

Fig. 2. Two reaction pathways, I and II, for the substitute reactions of H_2SiLiF with CH_3XH_{n-1} (X = F, Cl, Br, O, N; n = 1, 1, 1, 2, 3).

3.1. Substitution reactions of *A* with CH_3XH_{n-1} (X = F, Cl, Br, O, N; n = 1, 1, 1, 2, 3)

When CH_3XH_{n-1} approaches **A** with the end X of CH_3XH_{n-1} interacting on the positive Li atom of **A**, substitution reactions occur (see Fig. 1B). The calculation results indicate that there are two reaction pathways, I and II, for the substitution reactions of **A** with CH_3XH_{n-1} (see Fig. 2). Table 1 lists the total and relative energies together with the zero-point energies (ZPEs) of the stationary points. The term "relative energy" in the following means the energy of a species relative to the reactants in the same reaction. The calculated geometries of the stationary points in the path I are depicted in Fig. 3. Fig. 4 (for transition states **XSTS1**) and Supporting information (for other stationary points) show the structures of the stationary points in path II.

3.1.1. Path I

*3.1.1.1. Substitution reaction of **A** with CH_3Cl.* It is reasonable to expect that the first step in the **A** reaction with small molecules is the formation of a precursor complex (**ClSM1**). In **ClSM1**, the Li–Cl distance is 2.381 Å and the five atoms, Si, F, Li, Cl, C, lie in the same plane. Relative to two separated **A** and CH_3Cl molecules, there is little variation in the structural parameters of **A** and CH_3Cl moieties. However, the NBO calculations show that the transfer of electrons of the positive Li (natural charge: 0.856) in **A** to the negative Cl (natural charge: −0.080) in CH_3Cl does occur. Compared with those of **A** and CH_3Cl, the positive charge of the Li atom decreases

Table 1
Total energies (a.u.) and relative energies (kJ/mol, in parentheses) for reactants, intermediates, transition states and products of the substitution reactions at the B3LYP/6-311+G (d, p) level.

Molecules	*E*	ZPE	*E* + ZPE
A + CH_3F	−537.96277(0.0)	0.05793	−537.90842(0.0)
FSM1	−537.98602(−61.0)	0.05935	−537.92667(−47.9)
FSTS1	−537.94894(36.3)	0.05767	−537.89127(45.0)
FSTS2	−537.93728(66.9)	0.05682	−537.88046(73.4)
FSM2	−538.08769(−328.0)	0.06007	−538.02762(−313.0)
H_2SiFCH_3 + LiF	−538.00139(−10.3)	0.05830	−538.00139(−244.1)
A + CH_3Cl	−898.32318(0.0)	0.05662	−898.26662(0.0)
ClSM1	−898.34085 (−66.5)	0.05781	−898.28304(−43.1)
ClSTS1	−898.31701 (16.2)	0.05620	−898.26081(15.3)
ClSTS2	−898.29352(77.9)	0.05465	−898.23888(72.8)
ClSM2	−898.45344(−342.0)	0.05894	−898.39450(−335.7)
H_2SiFCH_3 + LiCl	−898.42527(−268.0)	0.05771	−898.36757(−265.0)
A + CH_3Br	−3012.24563(0.0)	0.05593	−3012.18970(0.0)
BrSM1	−3012.26262(−44.6)	0.05706	−3012.20556(−41.6)
BrSTS1	−3012.24296(7.0)	0.05561	−3012.18735(6.2)
BrSTS2	−3012.21688(75.5)	0.05426	−3012.16261(71.1)
BrSM2	−3012.37611(−342.6)	0.05873	−3012.31738(−335.2)
H_2SiFCH_3 + LiBr	−3012.34748(−267.4)	0.05754	−3012.28995(−263.2)
A + CH_3OH	−513.93638(0.0)	0.06996	−513.86642(0.0)
OSM1	−513.96927(−86.3)	0.07211	−513.89716(−80.7)
OSTS1	−513.90947(70.6)	0.06872	−513.84075(67.4)
OSTS2	−513.88888(124.7)	0.06736	−513.82152(117.9)
OSM2	−514.03172(−250.3)	0.07046	−513.96125(−249.0)
H_2SiFCH_3 + LiOH	−514.00879(−190.1)	0.06845	−513.94035(−194.1)
A + CH_3NH_2	−494.06528(0.0)	0.08271	−493.98257(0.0)
NSIM1	−494.10111(−94.1)	0.08524	−494.01588(−87.4)
NSTS1	−494.01921(120.9)	0.08107	−493.93814(116.7)
NSTS2	−493.99425(186.5)	0.07976	−493.91448(178.7)
NSIM2	−494.12202(−148.9)	0.08087	−494.04115(−153.8)
H_2SiFCH_3 + $LiNH_2$	−494.04257(−59.6)	0.07965	−494.01917(−96.1)

slightly, whereas the negative charge of the Cl atom increases by −0.038. The relative energy of **ClSM1** is 43.1 kJ/mol.

In **ClSM1**, the CH_3 moiety bears positive charges. As the reaction proceeds, the σ lone pair electrons of the Si atom attack the positive CH_3 from the opposite position of Cl (see Fig. 2 (path I)). Then the transition state **ClSTS1** forms. The natural charges of the Si atom increase evidently from 0.301 in **ClSM1** to 0.557 in **ClSTS1**. Thus silylenoid **A** shows nucleophilic behavior in the σ direction. IRC calculations (see Supporting information) indicate that, in the reaction process, the Si–C and C–Cl distances change largely. CH_3 leaves Cl to Si and the Si–C distance sharply shortens to 2.926 Å in **ClSTS1**. The interaction between Si and C atoms weakens the C···Cl interaction and the equilibrium bond distance of C–Cl is broken at about $s = -1.7$ (amu)$^{1/2}$ bohr. Relative to the sum of energies of **A** and CH_3Cl, the activation barrier is 15.3 kJ/mol.

After getting over the transition state **ClSTS1**, the Si–C and Li–Cl bonds gradually form with the rupture of C–Cl. The LiCl moiety separates away from the Si atom and the complex **ClSM2** forms. The process from **ClSTS1** to **ClSM2** is that of inversion of the triangular cone 'umbrella' formed by C and three H atoms. As a whole, this process is of S_N2-Si type nucleophilic substitution mechanism [51]. In fact, **ClSM2** is the complex of silane H_2SiFCH_3 and LiCl. The energy of **ClSM2** is lower than those of H_2SiFCH_3 and LiCl molecules by 70.7 kJ/mol. The energy needed for the dissociation of **ClSM2** is far less than that given out by the process from **ClSTS1** to **ClSM2** (351.0 kJ/mol). So there is enough energy in the reaction system to dissociate **ClSM2** into H_2SiFCH_3 and LiCl.

It can be found from the relative energies listed in Table 1 that the substitution reactions of **A** with CH_3Cl are exothermic. The value of reaction enthalpy is 265.0 kJ/mol.

*3.1.1.2. Substitution reactions of **A** with CH_3XH_{n-1} (X = F, Br, O, N; n = 1, 1, 2, 3).* The substitution reactions of **A** with CH_{3XHn-1} (X = F, Br, O, N; *n* = 1, 1, 2, 3) are similar to that of **A** with CH_3Cl.

All the precursor complexes **XSM1**, which are resulted from the Li···X interactions, display similar structures. The stability energies (relative to their corresponding reactants) of **XSM1** increase in the order of **BrSM1** (41.6 kJ/mol) < **ClSM1** (43.1 kJ/mol) < **FSM1** (47.9 kJ/mol) < **OSM1** (80.7 kJ/mol) < **NSM1** (87.4 kJ/mol).

All the transition states **XSTS1** are confirmed by calculation of the energy Hessian. As can be seen from Table 1, the energy of **FSTS1**, **ClSTS1**, **BrSTS1**, **NSTS1**, and **OSTS1** is 45.0, 15.3, 6.2, 67.4, and 116.7 kJ/mol higher than that of their corresponding reactants, and the activation energies from their corresponding precursor complexes are 92.9, 58.4, 47.8, 148.1, and 204.1 kJ/mol, respectively. One may therefore obtain the result that the barrier height decreases with the increase of the atomic number of X for the same

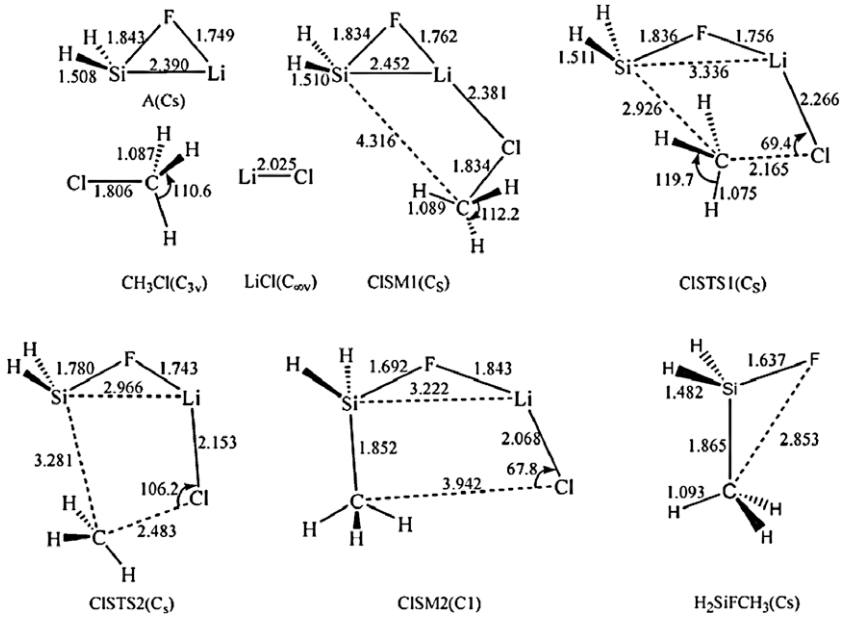

Fig. 3. The B3LYP/6-311+G (d, p) geometries (in Å and (°)) for the stationary points in the substitution reaction of H_2SiLiF with CH_3Cl.

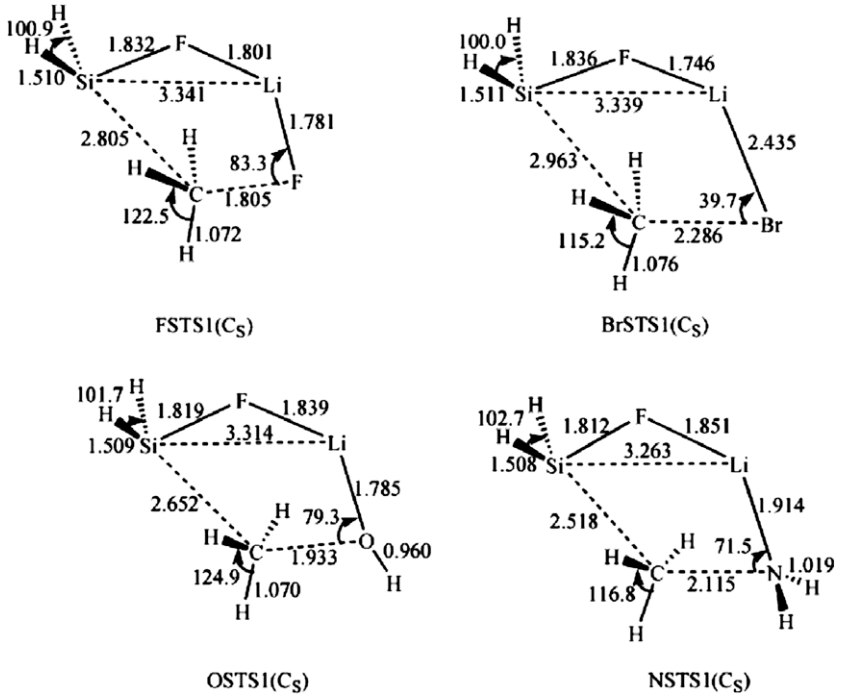

Fig. 4. The B3LYP/6-311+G (d, p) geometries (in Å and (°)) for the transition states **XSTS1** of path I in the substitution reactions of H_2SiLiF with CH_3XH_{n-1} (X = F, Br, O, N; n = 1, 1, 2, 3).

family systems or for the same period systems. Consequently, our theoretical results are in complete accord with the Hammond postulate [50], which associates a reactant-like transition state with a smaller barrier.

In the process from **XSTS1** to **XSM2**, the triangular cone 'umbrella' formed by C and three H atoms is inversed. Similar to that of **A** with CH_3Cl, the substitution processes are also of S_N2-Si type nucleophilic substitution mechanism for **A** with CH_3XH_{n-1} (X = F, Br, O, N; n = 1, 1, 2, 3) systems. Theoretical results (see Supporting information) indicate that all the substitution products **XSM2**, $(H)_2Si(F)(CH_3)(LiXH_{n-1})$, adopt a tetra-coordinate conformation on the silicon center. Our calculations show that **XSM2** can be considered a complex of silane H_2SiFCH_3 with compound $LiXH_{n-1}$. The predicted energy for the dissociation of **XSM2** (the maximum value is 72.0 kJ/mol) is far less than that given out by the process from **XSTS1** to **XSM2** (the minimum value is 289.8 kJ/mol). So the final products for the substitution reaction are H_2SiFCH_3 and $LiXH_{n-1}$.

As shown in Table 1, the substitution reactions of **A** with CH_3XH_{n-1} (X = F, Br, O, N; n = 1, 1, 2, 3) are exothermic. The enthalpy values are 244.1 (X = F), 263.2 (X = Br), 194.1 (X = O), 96.1 kJ/mol (X = N), respectively.

3.1.2. Path II

As shown in Fig. 1, the substitution path II of **A** with CH_3XH_{n-1} is same with path I in precursor complexes, product complexes and products. The only difference is that the structure of the transition state **XSTS2** (Fig. 5) is different from that of **XSTS1**.

*3.1.2.1. Substitution reaction of **A** with CH_3Cl.* After the formation of **ClSM1**, the σ electrons of the Si atom interact on the positive CH_3 group from the side of the Cl atom in CH_3Cl (see path II in Fig. 2), making the reaction proceed via path II. The optimized transition state **ClSTS2** is given in Fig. 3. Its only one imaginary frequency is 373.4i cm^{-1}. IRC calculations (see Supporting information) indicate the Si–C and C–Cl lengths change sharply and the triangular cone 'umbrella' formed by C and three H atoms is not reversed in the reaction process. Path II is similar to S_Ni-Si type nucleophilic substitution mechanisms [51]. If the H atoms in CH_3 are substituted by different atoms or groups, it is reasonable to expect that the product silanes obtained via paths I and II, respectively, would be enantiomers.

ClSTS2 and **ClSTS1** share similarities in that the five atoms, Si, F, Li, X, C, are in the same plane and the Li–X bond has been formed. The main differences between them are as follows: (1) In **ClSTS2**, the Si–C length is 3.281 Å, 0.355 Å longer than that in **ClSTS1**, indicating that the structure of **ClSTS1** is more similar to that of **ClSM2**. (2) The relative energy of **ClSTS2** is 72.8 kJ/mol (Table 1), which is 57.5 kJ/mol higher than that of **ClSTS1**. The higher energy of **ClSTS2** is probably due to that the Si atom gets larger repulsion from the negative Cl atom when the σ lone electrons of the Si atom attacks the CH_3 group from the same side of the Cl atom. It is apparent that path I is more favorable than path II.

*3.1.2.2. Substitution reactions of **A** with CH_3XH_{n-1} (X = F, Br, O, N; n = 1, 1, 2, 3).* In the cases of CH_3F, CH_3Br, CH_3OH, and CH_3NH_2, the silylenoid substitutions of path II are similar to that of the case CH_3Cl. The optimized transition states, **FSTS2**, **BrSTS2**, **OSTS2**, and **NSTS2** are depicted in Fig. 5. The energies of **FSTS2**, **ClSTS2**, **BrSTS2**, **OSTS2**, and **NSTS2** (Table 1) are above those of the reactants (**A** + CH_3XH_{n-1}) by 73.4, 72.8, 71.1, 117.9, and 178.7 kJ/mol, respectively. Also, the activation energies from the corresponding precursor complexes **XSM1** are in the order of **NSTS2** (266.1 kJ/mol) > **OSTS2** (198.6 kJ/mol) > **FSTS2** (121.3 kJ/mol) > **ClSTS2** (115.9 kJ/mol) > **BrSTS2** (112.7 kJ/mol). On this basis, one can therefore conclude that for the silylenoid substitution reaction with CH_3XH_{n-1} there is a very clear trend toward lower activation barriers for the element X on going from left to right along a given row and from upper down along a given column. This trend is same with that of path I.

The paths I and II share the same activation barrier trend for the substitution reactions of **A** with CH_3XH_{n-1} (X = F, Cl, Br, O, N; n = 1, 1, 1, 2, 3). The explanation for the activation barrier trend is con-

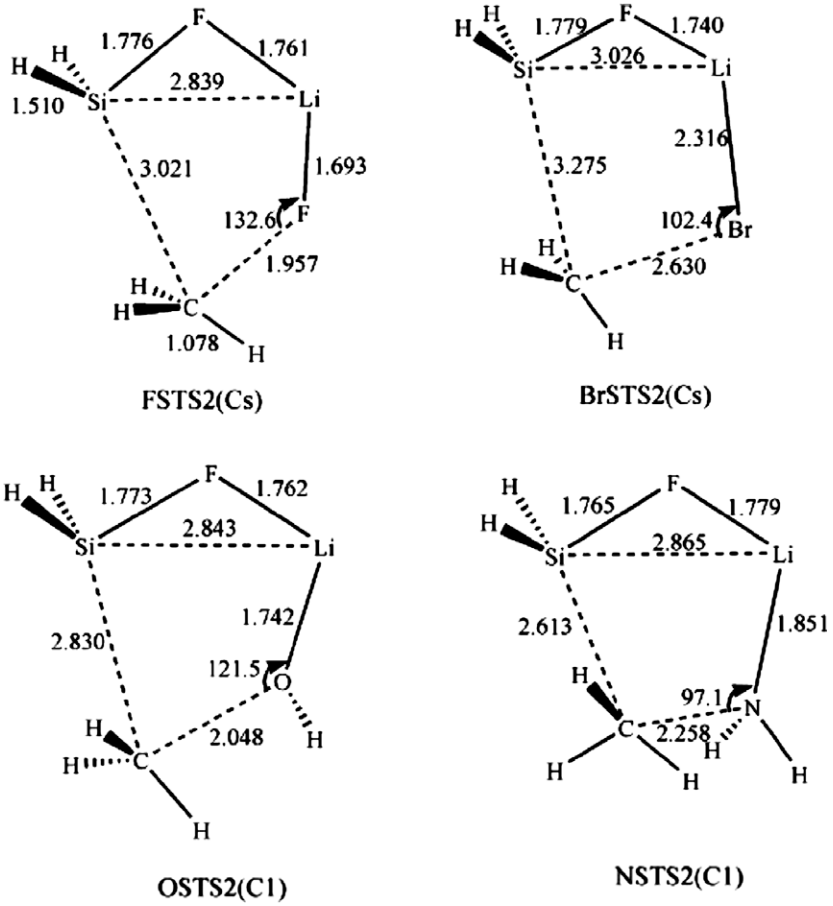

Fig. 5. The B3LYP/6-311+G (d, p) geometries (in Å and (°)) for the transition states **XSTS2** of path II in the substitution reactions of H_2SiLiF with CH_3XH_{n-1} (X = F, Br, O, N; n = 1, 1, 2, 3).

nected with the nature of CH_3XH_{n-1} and that of **A**. As can be seen in Fig. 2, the breaking of C–X bond and the making of Li–X bond are involved in the substitution reaction process. The strength of them becomes an important consideration. Table 2 lists the calculated bond energies of C–X in CH_3XH_{n-1} molecules and Li–X in the $LiXH_{n-1}$ molecules. The value of ΔE_X in Table 2 is the difference between the bond energies of C–X and Li–X. ΔE_X decreases in the order $\Delta E_N > \Delta E_O > \Delta E_F > \Delta E_{Cl} > \Delta E_{Br}$, which are in agreement with the trend of the barriers of the substitution reactions of **A** with CH_3XH_{n-1}. The result suggests that the values of ΔE_X concerning with the energies of C–X and Li–X may determine the preference of substitution reactions of **A** with CH_3XH_{n-1}.

3.1.2.3. Comparison between path I and path II. Both two substitution paths involve similar reaction processes and share same precursor complexes, product complexes and products. The main difference lies in the following aspects:

Table 2
The calculated bond energies (kJ/mol) of C–X in CH_3XH_{n-1} molecules and Li–X in the $LiXH_{n-1}$ molecules at the B3LYP/6-311+G (d, p) level (X = F, Cl, Br, O, N; n = 1, 1, 1, 2, 3).

X	E_{C-X}	E_{Li-X}	ΔE_X
F	500.6	554.2	−53.6
Cl	375.2	443.9	−68.7
Br	339.5	435.1	−95.6
O	434.2	404.5	29.7
N	411.0	204.4	206.6

$\Delta E_X = E_{C-X} - E_{Li-X}$.

(1) As shown in Fig. 2, the σ electrons of the Si atom attack the CH_3 group from the opposite side of the Cl atom in path I, whereas the Si atom attacks CH_3 from the same side of the Cl atom in path II. IRC calculations (see Supporting information) indicate the triangular cone 'umbrella' formed by C and three H atoms is reversed in path I, but it is not reversed in path II. As a whole, path I is similar to S_N2-Si type nucleophilic substitution mechanism with the inversion of conformation and path II is similar to S_Ni-Si type nucleophilic substitution mechanism with the retention of conformation. (2) As to the activation energies, the trend of path II is same with that of the path I. However, the energies of **XSTS2** are above those of **XSTS1** by 28.4 (X = F), 57.5 (X = Cl), 64.9 (X = Br), 50.5 (X = O), and 62.0 kJ/mol (X = N), respectively. That is, in the substitution reaction of **A** and CH_3XH_{n-1}, path I is more favorable than path II, and the superiority increases for the element X from upper down along a given column or from right to left along a given row. The possible explanation for this barrier difference is that the σ electrons of the Si atom suffer from more repulsion from XH_{n-1} in path II.

3.2. Insertion reactions of A into C–X (X = F, Cl, Br, O, N)

When CH_3XH_{n-1} approaches **A** with the X end of CH_3XH_{n-1} attacking the p-orbital of Si atom (see Fig. 1C), insertion reactions take place. Figs. 6 and 7 show the structures of some stationary points, and Supporting information lists orthogonal coordinates for others. The total energies together with the zero-point energies (ZPEs) and relative energies (relative to the corresponding reactants) of all stationary points are described by Table 3.

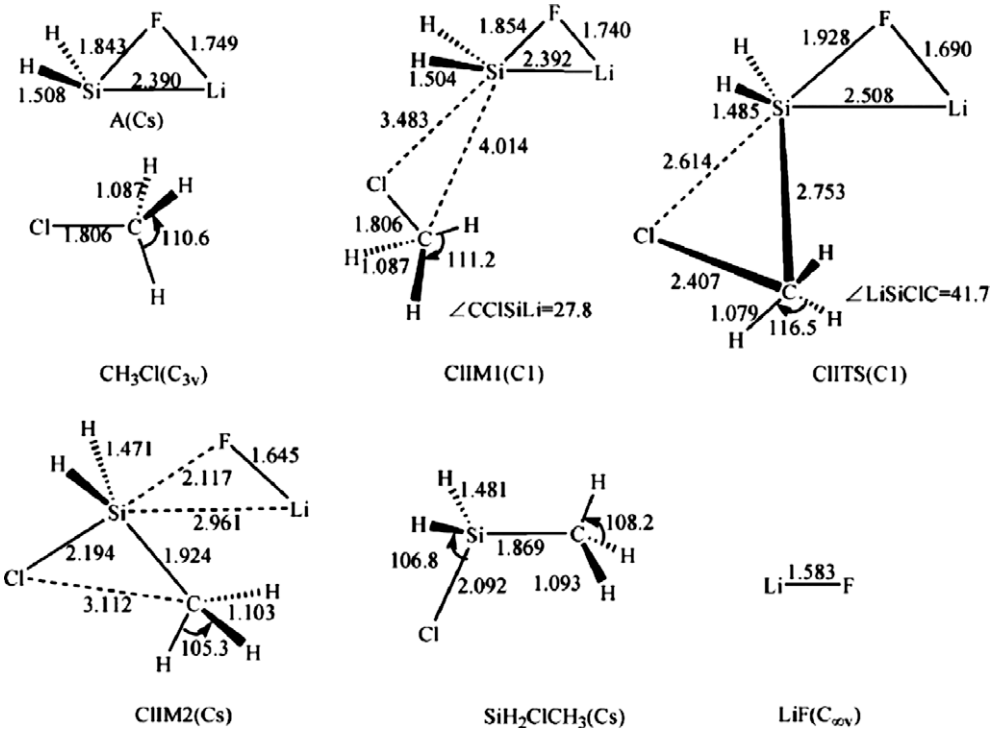

Fig. 6. The B3LYP/6-311+G (d, p) geometries (in Å and (°)) for the stationary points in the insertion reaction of H_2SiLiF with CH_3Cl.

*3.2.1. Insertion reaction of **A** into C–Cl*

In **A**, the p-orbital of the Si atom lied in the opposite situation of F is a part of LUMO. When CH_3Cl approaches **A**, the initial formation of the precursor complex **ClIM1** is facilitated by the interaction between the p-orbital on Si and the negative Cl atom of CH_3Cl. NBO analyses show that the electron donation of Cl into the p-orbital on the Si atom does occur. In comparison with those of **A** and CH_3Cl, the negative charge of the Cl atom and the positive charge of the Si atom decrease by 0.013 and 0.022, respectively. However, the long Si–Cl length (3.483 Å) in **ClIM1** and the small relative energy

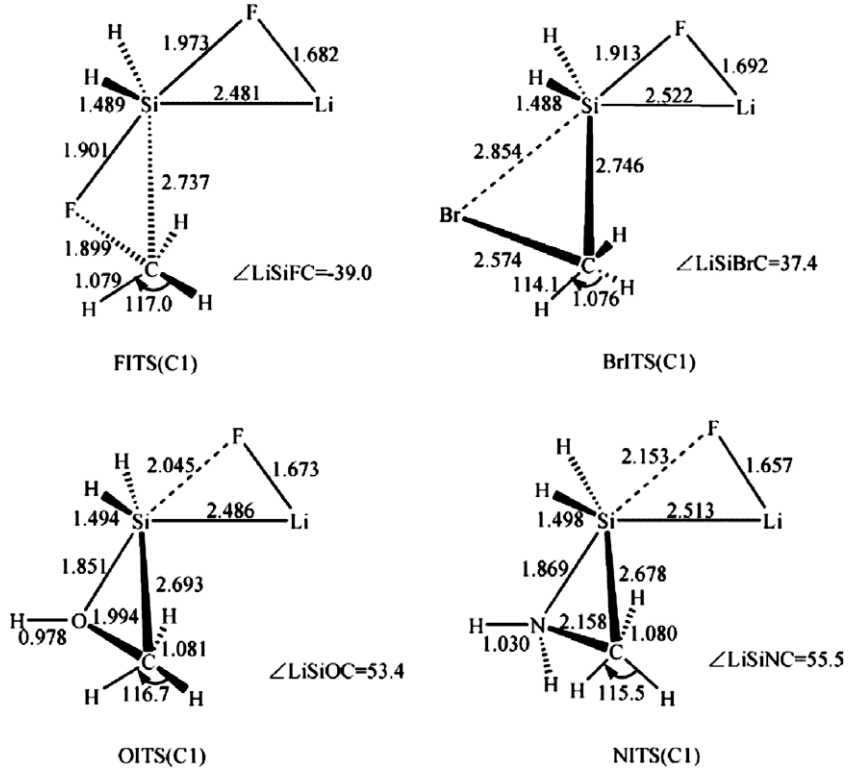

Fig. 7. The B3LYP/6-311+G (d, p) geometries (in Å and (°)) for the transition states **XITS** in the insertion reactions of H_2SiLiF and CH_3XH_{n-1} (X = F, Br, O, N; n = 1, 1, 2, 3).

Table 3
Total energies (a.u.) and relative energies (kJ/mol, in parentheses) for reactants, intermediates, transition states and products of the insertion reactions at the B3LYP/6-311+G (d, p) level.

Molecules	*E*	ZPE	*E* + ZPE
A + CH_3F	−537.96277(0.0)	0.05793	−537.90842(0.0)
FIM1	−537.96358(−1.6)	0.05888	−537.90470(−9.8)
FITS	−537.90179(160.1)	0.05733	−537.84445(168.0)
FIM2	−538.07217(−287.2)	0.06032	−538.01185(−271.6)
H_2SiCH_3F + LiF	−538.05969(−254.5)	0.05830	−538.00140(−244.1)
A + CH_3Cl	−898.32318(0.0)	0.05662	−898.26662(0.0)
ClIM1	−898.32400(−2.2)	0.05736	−898.26663(0.0)
ClITS	−898.25357(182.8)	0.05615	−898.19742(181.7)
ClIM2	−898.41237(−234.2)	0.05929	−898.35308(−227.0)
H_2SiCH_3Cl + LiF	−898.40068(−203.5)	0.05730	−898.34338(−201.5)
A + CH_3Br	−3012.24563(0.0)	0.05593	−3012.18970(0.0)
BrIM1	−3012.24638(−2.0)	0.05676	−3012.18962(0.2)
BrITS	−3012.17996(172.4)	0.05566	−3012.12430(171.7)
BrIM2	−3012.33152(−225.5)	0.05882	−3012.27271(−217.9)
H_2SiCH_3Br + LiF	−3012.31963(−194.3)	0.05687	−3012.26276(−191.8)
A + CH_3OH	−513.93638(0.0)	0.06996	−513.86642(0.0)
OIM1	−513.94179(−14.2)	0.07226	−513.86953(−8.2)
OITS	−513.86539(186.4)	0.06897	−513.79641(183.8)
OIM2	−514.02653(−236.7)	0.07119	−513.95533(−233.4)
H_2SiCH_3OH + LiF	−514.01938(−217.9)	0.08613	−513.95011(−219.7)
A + CH_3NH_2	494.06528(0.0)	0.08271	493.98257(0.0)
NIM1	−494.07948(−37.3)	0.08653	−493.99295(−27.3)
NITS	−493.98066(222.2)	0.08166	−493.89900(219.4)
NIM2	−494.13298(−177.7)	0.08220	−494.05078(−179.1)
$H_2SiCH_3NH_2$ + LiF	−494.12849(−166.0)	0.08088	−494.04760(−170.7)

of **ClIM1** (0.0 kJ/mol) indicate that the Si···Cl interaction is very weak.

As shown in Fig. 1, two electron donation effects contribute to the proceeding of the insertion reaction. One is the donation of the electrons of Cl into the p-orbital on the Si atom. The other is the donation of the σ electrons on the Si atom to the positive CH_3 group. The electron donations make the formation of the transition state **ClITS**, whose only one imaginary frequency is 524.0i cm^{-1}. In **ClITS**, the natural charge of the Si atom is 0.198 higher than that in **ClIM1**, while the natural charge of the CH_3Cl moiety decrease from the positive charge (0.015) in **ClIM1** to the negative charge (−0.261) in **ClITS**. This suggests that the Si atom has denoted electrons to the CH_3Cl moiety. The insertion reaction path was also fully confirmed by the IRC computations (see Supporting information). It is obvious that the bond lengths, Si–C, Si–Cl, and C–Cl, change strongly in the course of the reaction. The Si–C and Si–Cl bonds rapidly shorten from reactant side. The C–Cl bond sharply lengthens and the equilibrium bond length of C–Cl was broken at about $s = -5.2$ $(amu)^{1/2}$ bohr. The relative energy of **ClITS** is 181.7 kJ/mol.

After getting over the transition state **ClITS**, **ClIM2** are gradually formed with the LiF moiety leaving from the Si atom. In fact, **ClIM2** is a complex of $H_2SiClCH_3$ and LiF. The energy of **ClIM2** is 25.5 kJ/mol lower than the sum of the energies of $H_2SiClCH_3$ and LiF.

As shown in Table 3, the insertion reaction is exothermic by 201.5 kJ/mol for the **A** + CH_3Cl system.

3.2.2. insertion reactions of *A* into C–X (X = F, Cl, Br, O, N)

The insertion processes of **A** and CH_3XH_{n-1} (X = F, Br, O, N; n = 1, 1, 2, 3) are similar to that of **A** and CH_3Cl.

In the precursor complex **XIM1**, the Si–X distances are 2.902 (X = F), 3.590 (X = Br), 2.500 (X = O), and 2.236 Å (X = N), respectively. The energies of **XIM1** are lower than their corresponding reactants by 9.8 (X = F), 0.2 (X = Br), 8.2 (X = O), and 27.3 kJ/mol (X = N), respectively. The long Si–X distances and the small stability energies of **XIM1** indicate that there is only weak interaction between the Si atom and the X atom in **XIM1**, and **XIM1** is instable.

The transition states **XITS** are confirmed by calculation of the energy Hessian. The model calculations estimate that the relative energies of **FITS**, **BrITS**, **OITS**, **NITS** are 168.0, 171.7, 183.8, and 219.4 kJ/mol, respectively. That is, the reaction barriers of the insertions into C–X bonds increase for the same-row element X from right to left in the periodic table. This trend is same with that of silylenoid insertion into X–H of hydrides [14]. But the barriers of the silylenoid insertion into C–X bonds change very little (the maximum difference is 13.7 kJ/mol) for the same-family element X. Different from the insertion of silylene, silylenoid insertion reaction into C–Br is more favorable than that into C–Cl.

As can be seen in Fig. 1, the insertion process involves the breaking of C–X bond and the making of Si–C and Si–X bonds. Table 4 lists the bond energies of C–X in CH_3XH_{n-1} molecules, the bond energies of Si–C and Si–X in $H_2SiXH_{n-1}CH_3$. The results show that ΔE_X ($\Delta E_X = E_{C-X} - E_{Si-X} - E_{Si-C}$) decrease in the order of $\Delta E_N > \Delta E_{Cl} > \Delta E_{Br} > \Delta E_O > \Delta E_F$. It is clear that the ΔE_X is in the same order with the barrier trend of the silylenoid insertion reactions for the same period systems or for the same family systems. The result shows that the energies concerning with the C–X bond in CH_3XH_{n-1} and the Si–C and Si–X bonds in $H_2SiXH_{n-1}CH_3$ may determine the preference of insertion reactions of **A** into C–X bonds for the same-row element X or for the same-column element X.

The intermediate **XIM2** can further decompose to substituted silane $H_2SiCH_3XH_{n-1}$ and compound LiF. The energies of **XIM2** are below the sum of the energies of $H_2SiCH_3XH_{n-1}$ and LiF by 27.5 (X = F), 25.5 (X = Cl), 26.1 (X = Br), 13.7 (X = O), and 8.4 kJ/mol (X = N), respectively.

It is apparent that the reaction enthalpy for all the **A** insertions are 244.1 (C–F), 201.5 (C–Cl), 191.8 (C–Br), 219.7 (C–N), 170.7 kJ/mol (C–O), respectively.

3.3. Comparison between insertion and substitution reactions

To obtain a better understanding of the silylenoid insertion and substitution reactions, a comparison about the reaction mechanisms and energetics is made.

First, in these reactions, CH_3XH_{n-1} approaches **A** in different directions. In insertion reactions, the XH_{n-1} moiety of CH_3XH_{n-1} gets close to the Si atom of **A** from the opposite side of the F atom and results the interaction between the X atom and the Si atom. In substitution reactions, the XH_{n-1} moiety of CH_3XH_{n-1} approaches the Li atom from the opposite side of F and causes the Li···X interaction. The Si···X and Li···X interactions result in the formation of **XIM1** and **XSM1**, respectively. The Li···X interaction is stronger than the Si···X interaction due to that the positive charge of Li (0.856) is bigger than that of Si (0.306). So, **XSM1** is more stable than **XIM1**. This is confirmed by the DFT calculations that the energy of **XIM1** is above that of **XSM1** by 38.1 (X = F), 43.1 (X = Cl), 41.8 (X = Br), 72.5 (X = O), and 60.1 kJ/mol (X = N), respectively.

Second, the reaction barriers for the insertions are much higher than those for the substitutions. The total energies of **XITS** are

Table 4
The calculated bond energies (kJ/mol) of C–X in CH_3XH_{n-1} molecules, Si–C and Si–X in $H_2SiXH_{n-1}CH_3$ molecules at the B3LYP/6-311+G (d, p) level (X = F, Cl, Br, O, N; n = 1, 1, 1, 2, 3).

X	E_{C-X}	E_{Si-X}	E_{Si-C}	ΔE_X
F	487.5	607.0	415.6	−535.1
Cl	365.4	435.6	403.0	−473.2
Br	320.5	383.2	414.4	−477.1
O	421.6	497.4	415.8	−491.6
N	406.4	426.5	391.2	−411.3

$\Delta E_X = E_{C-X} - E_{Si-X} - E_{Si-C}$.

Table 5
Total energies (a.u.) and relative energies (kJ/mol, in parentheses) for reactants, intermediates, transition states and products of the substitution reactions in various solvents at the B3LYP/6-311+G (d, p) level.

Molecules	E_{ether} (ε = 4.3)	E_{THF} (ε = 7.6)	$E_{acetone}$ (ε = 20.7)
A + CH_3F	−537.91240(0.0)	−537.91483(0.0)	−537.92032(0.0)
FSM1	−537.94604(−88.3)	−537.94994(−92.2)	−537.95403(−88.5)
FSTS1	−537.91026(5.6)	−537.91411(1.9)	−537.91776(6.7)
FSTS2	−537.89561(44.1)	−537.89964(39.9)	−537.90289(45.8)
FSM2	−538.05866(−384.0)	−538.06453(−393.0)	−538.06986(−392.6)
H_2SiFCH_3 + LiF	−538.02325(−291.0)	−538.02775(−296.4)	−538.03372(−297.7)
A + CH_3Cl	−898.27266(0.0)	−898.27481(0.0)	−898.28003(0.0)
ClSM1	−898.30015(−72.2)	−898.30389(−76.3)	−898.30752(−72.2)
ClSTS1	−898.27717(11.8)	−898.28064(15.3)	−898.28403(10.5)
ClSTS2	−898.25379(49.5)	−898.25698(46.8)	−898.26008(52.4)
ClSM2	−898.42162(−391.0)	−898.42654(−398.3)	−898.43129(−397.1)
H_2SiFCH_3 + LiCl	−898.40237(−340.5)	−898.40904(−352.4)	−898.41529(−355.1)
A + CH_3Br	−3012.19558(0.0)	−3012.19769(0.0)	−3012.20286(0.0)
BrSM1	−3012.22250(−70.7)	−3012.22622(−74.9)	−3012.22981(−70.8)
BrSTS1	−3012.20301(19.5)	−3012.20637(22.8)	−3012.20963(17.8)
BrSTS2	−3012.17682(49.2)	−3012.17990(46.7)	−3012.18293(52.3)
BrSM2	−3012.34268(−386.2)	−3012.34737(−392.9)	−3012.35183(−391.1)
H_2SiFCH_3 + LiBr	−3012.32323(−335.1)	−3012.32967(−346.4)	−3012.33575(−348.8)
A + CH_3OH	−513.87704(0.0)	−513.88027(0.0)	−513.88661(0.0)
OSM1	−513.91913(−110.5)	−513.92395(−114.7)	−513.92776(−108.0)
OSTS1	−513.85731(51.8)	−513.86113(50.2)	−513.86478(57.3)
OSTS2	−513.83569(108.5)	−513.83889(108.6)	−513.84134(118.8)
OSM2	−513.98802(−291.3)	−513.99310(−296.2)	−513.99801(−292.4)
H_2SiFCH_3 + LiOH	−513.95601(−207.3)	−513.95965(−208.4)	−513.96488(−205.5)
A + CH_3NH_2	−493.99154(0.0)	−493.99443(0.0)	−494.00072(0.0)
NSM1	−494.03737(−120.3)	−494.04172(−124.1)	−494.04578(−118.3)
NSTS1	−493.95164(104.7)	−493.95450(104.8)	−493.95758(113.2)
NSTS2	−493.92543(173.5)	−493.92773(175.1)	−493.93003(185.6)
NSM2	−494.06416(−190.6)	−494.06898(−195.7)	−494.07330(−190.6)
H_2SiFCH_3 + $LiNH_2$	−494.03260(−107.8)	−494.03576(−108.5)	−494.04094(−105.6)

(123.0, 94.6) (X = F), (166.4, 108.9) (X = Cl), (165.5, 100.6) (X = Br), (116.4, 65.9) (X = O), and (102.7, 40.7) kJ/mol (X = N) higher than those of the corresponding **XSTS1**, **XSTS2**, respectively. On this base, one may therefore conclude that the substitution reactions are more favorable than the insertion reactions for the **A** and CH_3XH_{n-1} systems.

Third, the final products of the substitution reactions are H_2SiFCH_3 and $LiXH_{n-1}$, while $H_2SiXH_{n-1}CH_3$ and LiF are finally obtained from the insertion reactions. Therefore, H_2SiFCH_3, $H_2SiXH_{n-1}CH_3$ and LiX perhaps present in the CH_3XH_{n-1} and **A** reaction systems. It is reasonable to expect that among the final products, the amount of H_2SiFCH_3 is more than that of $H_2SiXH_{n-1}CH_3$ due to the superiority of the substitution reaction over the insertion reaction. When the insertion barrier is higher enough than the substitution barrier, insertion product $H_2SiXH_{n-1}CH_3$ could not form. In Gregory Molev's experiments [24], the substitution product **2**, instead of insertion product **3**, was obtained, indicating that the substitution process is the main reaction process of fluorosilylenoid 1 and CH_3Cl. Our theoretical findings are in accord with this experiment.

Fourth, both the insertion and substitution reactions of **A** with CH_3XH_{n-1} are exothermic.

3.3.1. Solvent effects on substitution reactions

According to the above discussion, the substitution reactions take priority over the insertion reactions for **A** and CH_3XH_{n-1} systems. So the solvent effects on the substitution reaction are investigated. Three solvents, ether, THF and acetone, are chosen for the study.

Similar to the reactions in vacuum, there are two pathways for the substitution reactions in solvents. The geometry structures (see Supporting information) of stationary points in solvents (ether, THF and acetone, respectively) are correspondingly similar to those in vacuum. Calculated energies of them are listed in Tables 5 and 6. Several conclusions can be drawn from these calculations. (1) Energies of all stationary points are in the order of $E_{acetone} < E_{THF} < E_{ether} < E_{vacuum}$, indicating that the thermal stabilities of the stationary points are larger in solvents than in vacuum, and increase with the polarities of solvents. (2) With the exceptions of path I for the case of CH_3Br and path II for the cases of CH_3NH_2 and CH_3OH in acetone, the energy barriers in vacuum are higher than those in solvents, showing that in these conditions, substitution reactions are easy to occur in solvents. (3) The energy barriers change very little (the maximum difference is 10.5 kJ/mol, which is

Table 6
The energies (kJ/mol) of all transition states relative to those of their corresponding reactants for the substitution reactions at the B3LYP/6-311+G (d, p) level.

TS	ΔE^* in vacuum	ΔE^* in ether	ΔE^* in THF	ΔE^* in acetone
FSTS1	45.0	5.6	1.9	6.7
FSTS2	73.4	44.1	39.9	45.8
ΔE_F^*	28.4	38.5	38.0	39.1
ClSTS1	15.3	11.8	15.3	10.5
ClSTS2	72.8	49.5	46.8	52.4
ΔE_{Cl}^*	57.5	37.7	31.5	41.9
BrSTS1	6.2	19.5	22.8	17.8
BrSTS2	71.1	49.2	46.7	52.3
ΔE_{Br}^*	64.9	29.7	23.9	34.5
OSTS1	67.4	51.8	50.2	57.3
OSTS2	117.9	108.5	108.6	118.8
ΔE_O^*	50.5	56.7	58.4	61.5
NSTS1	116.7	104.7	104.8	113.2
NSTS2	178.7	175.3	175.1	185.6
ΔE_N^*	62.0	70.6	70.3	72.4

$\Delta E_X^* = \Delta E_{\mathbf{XSTS2}} - \Delta E_{\mathbf{XSTS1}}$ (X = F, Cl, Br, O, N).

for the cases of CH_3NH_2 in THF and in acetone) with the solvent polarity, suggesting that the solvent polarity has little effects on the reactions. (4) Whether in vacuum or in solvents, the energy of **XSTS1** is lower than that of the corresponding **XSTS2**, indicating that path I take priority over path II. The difference between **XSTS1** and **XSTS2** in solvents is bigger than that in vacuum for the X = F, O, N cases, whereas the cases of X = Cl, Br are in opposite conditions. (5) The barrier heights for the main substitution path I in solvents increase in the order $CH_3F < CH_3Cl < CH_3Br < CH_3OH < CH_3NH_2$. That is, for silylenoid substitutions in solvents there is a very clear trend toward higher barriers with the element X on going from right to left in a given row or from the top down in a given column. Compared with those in vacuum, the barrier heights in solvents are in the same order for the same row systems, whereas in reverse order for the same family systems. (6) Same with those in vacuum, H_2SiFCH_3 and $LiXH_{n-1}$ are expected final products for the substitution reactions in solvents. (7) It is apparent that all the silylenoid substitutions are thermodynamically exothermic. The reaction enthalpy changes very little with the polarity of the solvent.

4. Concluding remarks

In the present work, we have studied the reaction mechanisms of silylenoid H_2SiLiF substitutions and insertions with CH_3XH_{n-1} (X = F, Cl, Br, O, N; n = 1, 1, 1, 2, 3) by DFT theory. It should be mentioned that this study has provided the first theoretical demonstration about the reaction trajectory and theoretical estimation of the activation energy and reaction enthalpy for those processes. The calculated results are in agreement with experiments.

1. The theoretical results indicate that the substitution reactions of **A** with CH_3XH_{n-1} occur in a concerted manner via two reaction paths, I and II, forming same products, H_2SiFCH_3 and $LiXH_{n-1}$. For both pathways, the substitution barriers of **A** with CH_3XH_{n-1} decrease with the increase of the atomic number of the element X for the same family systems or for the same row systems. Path I is more favorable than path II.
2. **A** inserts into a C–X bond via a concerted manner, forming $H_2SiXH_{n-1}CH_3$ and LiF. For C–X bonds, the order of reactivity by **A** insertion indicates the reaction barriers increase for the same-row element X from right to left in the periodic table, whereas change very little for the insertion into X–C bonds of the same-family element X.
3. The XH_{n-1} moiety of CH_3XH_{n-1} getting close to Si and Li atoms of **A** causes the insertion and substitution reactions, respectively. The total energies of the insertion transition states **XITS** are higher than those of the corresponding substitution states **XSTS1**, **XSTS2**, respectively. Thus, the substitution reactions are more favorable than the insertion reactions for the **A** and CH_3XH_{n-1} systems. It is reasonable to expect that the amount of substitute product H_2SiFCH_3 is more than that of insertion product $H_2SiXH_{n-1}CH_3$ among the final products. Both the insertion and substitution reactions of **A** with CH_3XH_{n-1} are exothermic.
4. In solvents, the substitution reaction process of **A** with CH_3XH_{n-1} is similar to that in vacuum. The barrier heights in solvents increase in the order $CH_3F < CH_3Cl < CH_3Br < CH_3OH < CH_3NH_2$. The solvent polarity has little effects on the substitution barriers.

Acknowledgements

This work was supported financially by the National Nature Science Foundation of China (No. 20574043).

Appendix A. Supplementary material

Supplementary data associated with this article can be found, in the online version, at doi:10.1016/j.jorganchem.2008.12.017.

References

[1] H. Gilman, D.J. Peterson, J. Am. Chem. Soc. 87 (1965) 2389.
[2] O.M. Nefedow, M.N. Manakow, Angew. Chem. 76 (1964) 270.
[3] D.C. Feng, S.Y. Feng, C.H. Deng, Chem. J. Chin. Univ. 17 (1995) 1108.
[4] S.Y. Feng, Y.F. Zhou, D.C. Feng, J. Phys. Chem. A 107 (2003) 4116.
[5] Y. Qi, D. Feng, S. Feng, J. Mol. Struct. (Theochem.) 856 (2008) 96.
[6] Driver, G. Tom, K.A.J. Woerpel, Am. Chem. Soc. 126 (2004) 9993.
[7] P.B. Glaser, T.D. Tilley, J. Am. Chem. Soc. 125 (2003) 13640.
[8] B. Gehrhus, P.B. Hitchcock, M. Lappert, Organometallics 16 (1997) 4861.
[9] R. Becerra, J.P. Cannady, R. Walsh, J. Phys. Chem. A 103 (1999) 4457.
[10] P.N. Skancke, J. Phys. Chem. A 101 (1997) 5017.
[11] R. Becerra, J.P. Cannady, R. Walsh, J. Phys. Chem. A 106 (2002) 11558.
[12] W. Ando, M. Ikeno, A. Sekiguchi, J. Am. Chem. Soc. 99 (1977) 6447.
[13] W. Ando, K. Haglwara, A. Sekiguchi, Organometallics 6 (1987) 2270.
[14] J. Xie, D. Feng, S. Feng, J. Organomet. Chem. 691 (2006) 208.
[15] J. Xie, D. Feng, S. Feng, J. Zhang, J. Mol. Struct. (Theochem.) 755 (2005) 55.
[16] S. Feng, D. Feng, J. Li, Chem. Phys. Lett. 316 (2000) 146.
[17] S. Feng, C. Deng, Chem. Phys. Lett. 186 (1991) 248.
[18] L.E. Bourque, P.A. Cleary, K.A. Woerpel, J. Am. Chem. Soc. (Commun.) 129 (2007) 12602.
[19] K.P. Steele, W.P. Weber, Inorg. Chem. 20 (1981) 1302.
[20] K. Raghavachari, J. Chandrasekhar, M.J. Frisch, J. Am. Chem. Soc. 104 (1982) 3779.
[21] K. Raghavachari, J. Chandrasekhar, M.S. Gordon, K. Dykema, J. Am. Chem. Soc. 106 (1984) 5853.
[22] D.F. Moser, T. Bosse, J. Olson, J.L. Moser, I.A. Guzei, R. West, J. Am. Chem. Soc. 124 (2002) 4186.
[23] M.D. Su, J. Am. Chem. Soc. 125 (2003) 1714.
[24] G. Molev, D. Bravo-Zhivotovskii, M. Karni, B. Tumanskii, M. Botoshansky, Y. Apeloig, J. Am. Chem. Soc. (Commun.) 128 (2006) 2784.
[25] A.D. Beck, J Chem. Phys. 98 (1993) 5648.
[26] A.D. Beck, Phys. Rev. A 38 (1988) 3098.
[27] S.H. Vosko, L. Wilk, M. Nusair, Can. J. Phys. 58 (1980) 1200.
[28] C. Lee, W. Yang, R.G. Parr, Phys. Rev. B 37 (1988) 785.
[29] J.P. Foster, F. Weinhold, J. Am. Chem. Soc. 102 (1980) 7211.
[30] A.E. Reed, F. Weinhold, J. Chem. Phys. 78 (1983) 4066.
[31] F. Weinhold, in: P.V.R. Schleyer (Ed.), Encyclopedia of Computational Chemistry, vol. 3, 1998, pp. 1792–1811.
[32] L.A. Curtiss, P.C. Redfern, K. Raghavachari, V. Rassolov, J.A. Pople, J. Chem. Phys. 110 (1999) 4703.
[33] S. Miertus, E. Scrocco, J. Tomasi, Chem. Phys. 55 (1981) 117.
[34] S. Miertus, J. Tomasi, Chem. Phys. 65 (1982) 239.
[35] M. Cossi, V. Barone, R. Cammi, J. Tomasi, Chem. Phys. Lett. 255 (1996) 327.
[36] M.T. Cancès, B. Mennucci, J. Tomasi, J. Chem. Phys. 107 (1997) 3032.
[37] V. Barone, M. Cossi, J. Tomasi, Chem. Phys. 107 (1997) 3210.
[38] M. Cossi, V. Barone, B. Mennucci, J. Tomasi, Chem. Phys. Lett. 286 (1998) 253.
[39] V. Barone, M. Cossi, J. Tomasi, J. Comput. Chem. 19 (1998) 404.
[40] V. Barone, M. Cossi, J. Phys. Chem. A 102 (1998) 1995.
[41] B. Mennucci, J. Tomasi, J. Chem. Phys. 106 (1997) 5151.
[42] J. Tomasi, B. Mennucci, E. Cancès, J. Mol. Struct. (Theochem.) 464 (1999) 211.
[43] M.J. Frisch, G.W. Trucks, H.B. Schlegel, G.E. Scuseria, M.A. Robb, J.R. Cheeseman, J.A. Montgomery, N.J. Vreven, T.K. Kudin, J.C. Burant, J.M. Millam, S.S. Iyengar, J.B. Tomasi, V. Mennucci, B.M. Cossi, G. Scalmani, N. Rega, G.A. Petersson, H. Nakatsuji, M. Hada, M. Ehara, K. Toyota, R. Fukuda, J. Hasegawa, M. Ishida, T. Nakajima, Y. Honda, O. Kitao, H. Nakai, M. Klene, X. Li, J.E. Knox, H.P. Hratchian, J.B. Cross, V. Bakken, C. Adamo, J. Jaramillo, R. Gomperts, R.E. Stratmann, O. Yazyev, A.J. Austin, R. Cammi, C. Pomelli, J.W. Ochterski, P.Y. Ayala, K. Morokuma, G.A. Voth, P. Salvador, J.J. Dannenberg, V.G. Zakrzewski, S. Dapprich, A.D. Daniels, M.C. Strain, O. Farkas, D.K. Malick, A.D. Rabuck, K. Raghavachari, J.B. Foresman, J.V. Ortiz, Q. Cui, A.G. Baboul, S. Clifford, J. Cioslowski, B.B. Stefanov, G. Liu; A. Liashenko, P. Piskorz, I.R. Komaromi, L.D. Martin, J. Fox, T. Keith, M.A. AlLaham, C.Y. Peng, A. Nanayakkara, M. Challacombe, P.M. Gill, W.B. Johnson, W. Chen, M.W. Wong, C. Gonzalez, J.A. Pople, Gaussian 03, Revision, Gaussian, Inc., Pittsburgh PA, 2003.
[44] T. Clark, P.R. Schleyer, J. Organomet. Chem. 191 (1980) 347.
[45] S. Feng, D. Feng, C. Deng, Chem. Phys. Lett. 214 (1993) 97.
[46] S. Feng, D. Feng, J. Mol. Struct. (Theochem.) 541 (2001) 171.
[47] D. Feng, J. Xie, S. Feng, Chem. Phys. Lett. 396 (2004) 245.
[48] S. Feng, G. Ju, C. Deng, Sic. Chin. (Ser. B) 35 (1992) 523.
[49] S. Feng, D. Feng, C. Deng, Chin. J. Chem. 13 (1995) 19.
[50] L.H. Sommer, C.M. Golino, D.N. Roark, R.D. Bush, J. Organomet. Chem. 49 (1973) C13.
[51] G.S. Hammond, J. Am. Chem. Soc. 77 (1955) 334.